Contrib. Astron. Obs. Skalnaté Pleso **52/3**, 116 – 125, (2022)
https://doi.org/10.31577/caosp.2022.52.3.116

Influence of the solar hydrogen Lyα line on the GNSS signal delay in the ionospheric D-region

D. Petković[1], **O. Odalović**[1] **and A. Nina**[2]

[1] *Faculty of Civil Engineering, University of Belgrade, Bulevar kralja Aleksandra 73, 11000 Belgrade, Serbia*

[2] *Institute of Physics Belgrade, University of Belgrade, Pregrevica 118, 11080 Belgrade, Serbia (E-mail: sandrast@ipb.ac.rs)*

Received: July 20, 2022; Accepted: October 2, 2022

Abstract. Recent research indicates that the influence of the ionospheric D-region on the propagation of satellite signals cannot be ignored during the intense X-radiation emitted during solar X-ray flares. In this paper, we investigate the influence of changes in the solar hydrogen Lyα radiation, which is manifested in variations of the D-region electron density and, consequently, the total electron content in this region, on the propagation of the Global Navigation Satellite System (GNSS) signals. We consider changes during a solar cycle and year, represented by the smoothed daily sunspot number and the day of year. The obtained results indicate that the influence of the D-region on these signals is not negligible for positioning with a single signal recorded by a single receiver during the period around the maximum of a solar cycle.

Key words: solar hydrogen Lyα radiation – total electron content – ionosphere – GNSS signal delay

1. Introduction

The terrestrial atmosphere is constantly exposed to the influence of solar radiation, which significantly affects the characteristics of its upper part. The consequence of that influence is the formation of the ionized layer called the ionosphere (50 km - 1000 km) in which ionization processes occur in collisions of atmospheric particles with different kinds of particles and photons. Photo-ionization processes depend on the incident photons wavelengths and the considered location. Namely, solar photons in the upper ionosphere, which play a dominant role in photo-ionization processes in these altitude domain, have wavelengths in the soft X-domain of the electromagnetic spectrum, while, during quiet solar conditions, the solar hydrogen Lyα photons are the most significant source of these processes in the lowest ionospheric layer called the D-region.

Free electrons produced in the photo-ionization processes play a significant role in the propagation of electromagnetic waves, including the satellite signals emitted by the Global Navigation Satellite System (GNSS). This system refers

to any constellation of satellites used to provide accurate and three-dimensional positioning and navigation on a global or regional scale. The United States Department of Defense has been established NAVSTAR GPS (Global Positioning System) as the very first system of its kind. Following that lead, five other positioning systems were built during the last two decades, including Russia's Global Navigation Satellite System (GLONASS), China's BeiDou (or COMPASS), the Navigation with Indian Constellation (NavIC) (or the Indian Regional Navigation Satellite System (IRNSS)), Japanese Quasi-Zenith Satellite System (QZSS), and the European Union's GALILEO (Hofmann-Wellenhof et al., 2008).

GNSS signals play a very important role in modern life, which is why the study of the ionospheric electron density changes also has practical applications. The influence of the atmosphere on their propagation is significant in the ionosphere and troposphere. At the same time, the ionospheric effect on signal propagation is more important in the upper ionosphere due to a significantly higher electron density than at its lower altitudes. However, recent research indicates that the influence of the perturbed D-region cannot be ignored (Nina et al., 2020). Bearing in mind that even in the absence of sudden disturbances, the characteristics of this ionospheric layer change significantly due to changes in the intensity of incoming Lyα radiation during a solar cycle, year and time of day, the question arises as to how these changes affect the propagation of a GNSS signal. The aim of this paper is to investigate the influence of changes in Lyα radiation during a solar cycle on the delay of the GNSS signal during a year. In this study, we analyse the maximum daily influence of the D-region on the signals, which occurs at noon. This analysis is based on Wait's model of the ionosphere (Wait & Spies, 1964), which describes the ionosphere with two parameters: the "sharpness", β and the signal reflection height, H', and on the Quiet Ionospheric D-Region (QIonDR) model (Nina et al., 2021), which provides these parameters at noon of the selected day. According to the QIonDR model, White's parameters are counted as functions of the ordinal number of this day in year (Day of Year, DOY) and the smoothed daily sunspot number, σ, relevant for the considered day.

2. Modelling

The solar ionizing radiation (particles and photons in the soft X and UV domains) produces the free electrons in the ionosphere in sufficient quantities to directly affect the radio waves propagation (from 3 kHz up to 300 GHz). The ionospheric parameter which has a significant role in quantification of the ionosphere's state impact on the electromagnetic wave propagation is the Total Electron Content (TEC). It represents the total number of electrons in a column with a 1 m^2 cross-section area along the signal path from a transmitter

(satellite) to the receiver. Thus, it can be expressed by the simple line integral (Seeber, 2003; Hofmann-Wellenhof et al., 2008):

$$TEC(t) = \int_S^R N_e \, dh, \tag{1}$$

in which N_e stands for the electron density, R and S are the upper and lower ionosphere boundary, and h is the altitude. TEC is expressed in the Total Electron Content Units (TECU), which amounts to 10^{16} free electrons per m^2.

TEC delays signal propagation from satellite to receiver. Relationship between TEC and signal delay (P_{ION}) is defined by following equation (Hofmann-Wellenhof et al., 2008):

$$P_{ION} = \pm \frac{40.3}{f^2} \cdot \int_S^R N_e \, dh = \pm \frac{40.3}{f^2} \cdot TEC, \tag{2}$$

where f denotes frequency of the considered electromagnetic wave, i.e. the used satellite signal.

In this paper, we focus attention on the D-region influence on the signal propagation. For this reason, we modify Equations (1) and (2) such that they only apply to this ionospheric region. If we slightly modify integration boundaries, by setting the upper and lower bounds of the D region instead, i.e. $S = h_{low} = 60\,\mathrm{km}$ and $R = h_{upp} = 90\,\mathrm{km}$, Equation (1) can be rewritten as follows:

$$TEC_D(t) = \int_{h_{low}}^{h_{upp}} N_e \, dh, \tag{3}$$

where index D in TEC_D indicates that the TEC value is for ionospheric D-region. In a manner that is analogous to the example given earlier, we are going to refer to the signal delay in the D-region as P_D:

$$P_D = 40.3 \, \frac{TEC_D}{f^2}. \tag{4}$$

It is necessary to point out that Equations (1) and (3) represents the TEC calculation for the electromagnetic wave that is coming in from the zenith direction (signal path goes perpendicular to the D-region boundary). In the case that the satellite signal does not arrive from the zenith direction, slant TEC ($STEC$ or $STEC_D$ for D-region only) is introduced. $STEC$ can be calculated using the vertical TEC value and the mapping function $S(\theta)$ corresponding to the actual zenith angle θ:

$$STEC_D(t) = S(\theta) \cdot TEC_D(t) = \frac{TEC_D(t)}{cos(\theta)}. \tag{5}$$

As can be seen Equation (3), the TEC in both the vertical and slant directions is a function of the electron density N_e. Equation that can be used to calculate the electron density is as follows (Thomson, 1993):

$$N_e(\beta, H', h) = 1.43 \cdot 10^{13} \cdot e^{-\beta \cdot H'} \cdot e^{[\beta - 0.15]h}, \tag{6}$$

where the "sharpness", β, and the signal reflection height, H', are given in km^{-1} and km, respectively. For quiet solar conditions, these parameters can be determined using the expressions developed in (Nina et al., 2021) for the Central Europe using the Quiet Ionosphere D-region (QIonDR) Model. β can be obtained from:

$$\begin{aligned} \beta(\sigma, \chi) = 0.2635 + 0.002573 \cdot \sigma - 9.024 \cdot 10^{-6} \cdot \sigma^2 \\ +0.005351 \cdot cos(2\pi(\chi - 0.4712)). \end{aligned} \tag{7}$$

while H' can be calculated as:

$$H'(\sigma, \chi) = 74.74 - 0.02984 \cdot \sigma + 0.5705 \cdot cos(2\pi(\chi - 0.4712) + \pi). \tag{8}$$

As one can see in previous expressions, both, β and H', depend on the two parameters which represent dependency on a solar cycle period, described in terms of the smoothed daily sunspot number, σ, and dependency on the season parameter $\chi = DOY/365$, where DOY is the day of year (Nina et al., 2021).

The following expression, derived from Equations (3) and (6), can be used to calculate the TEC value in the D-region (Todorović Drakul et al., 2016):

$$TEC_D(t) = 1000 \, \frac{N_e(\beta, H', h_t) - N_e(\beta, H', h_t)}{\beta(\sigma, \chi) - 0.15}. \tag{9}$$

As one can see, the signal delay, P_D, is a function of the seasonal parameter, χ, smoothed daily sunspot number, σ, zenith angle from which electromagnetic wave reached ionospheric layer, θ, and frequency of the considered signal f. In this study, we analyse the dependencies on χ and σ for the three fixed values of θ, and the two f which are used for satellite signals important for the GNSS positioning.

In addition to analysis of P_D dependencies of the indicated parameters, we also provide analysis of its changes with σ (i.e. changes of derivative $\frac{\Delta P_D}{\Delta \sigma}$) depending on the same parameters.

3. Results and discussion

In this contribution, we calculated signal delay P_D for TEC values as function of DOY and the smoothed daily sunspot number. The values of the zenith angles are chosen to cover the best and worst case scenarios regarding the application of GNSS technology - zenith angle values of $\theta = 0°$ and $\theta = 70°$, as well as

their mean value $\theta = 35°$. Calculations of TEC values are performed to cover all seasons and values of smoothed daily sunspot number σ in the range of 20 to 120. Fig. 1 illustrates vertical TEC values. It shows that TEC reaches its peak during the summer months (summer solstice), and increases with σ.

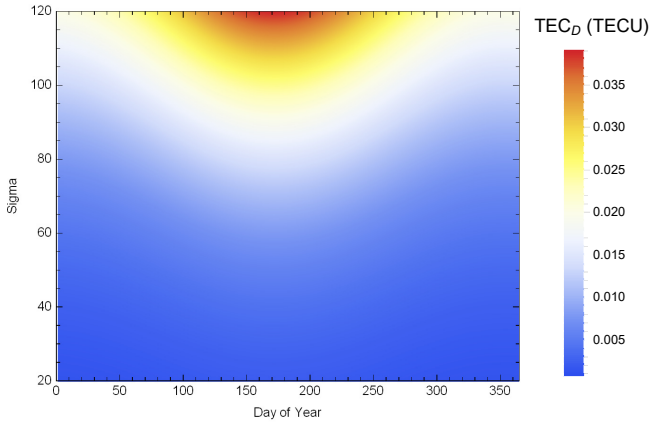

Figure 1. Dependency of vertical TEC_D on the day of year and σ values.

Calculations of the slant TEC are performed based on vertical TEC values and Equation (5). Fig. 2 illustrates those values for zenith angle of $\theta = 35°$ and $\theta = 70°$, respectively. The maximum TEC values for θ values of 0°, 35°, and 70° are respectively 0.04, 0.05, and 0.11 TECU. According to those, we shown that values grow as the zenith angle increases (e.g. as satellite reaches horizon).

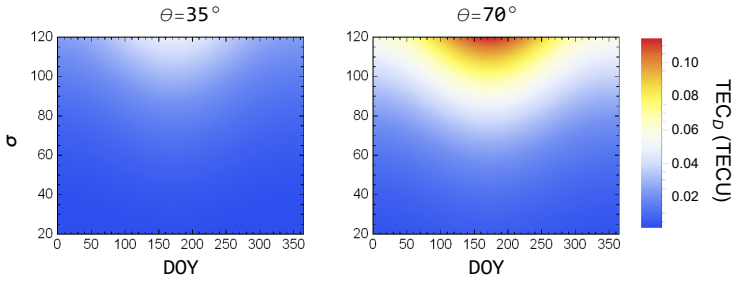

Figure 2. Dependency of the slant TEC_D on the day of year, DOY, and the smoothed daily sunspot number, σ, for the zenith angles $\theta = 35°$ (left) and $\theta = 70°$ (right).

In addition to the TEC values, we analyse the signal delay due to influence of the ionospheric D-region. We consider the frequencies used to broadcast satellite

signals of the satellite systems mentioned in Introduction which are in the range of approximately 1.2 GHz to 1.6 GHz (Hofmann-Wellenhof et al., 2008). In this study we provide calculations for $f_1 = 1.2$ GHz and $f_2 = 1.6$ GHz.

The calculated delays are presented in Fig. 3. In the case of the frequency f_2, signal delay reached values of 6 mm, 8 mm, and 18 mm for $\theta = 0°$, 35°, and 70°. Within the same spirit, for the frequency f_1, correspondent delay values are 11mm, 13 mm, and 32 mm. The comparison of the signal delays for the used frequencies are given in the third row of Fig. 3. Analysing this comparison, we can conclude that, even in a relatively small considered frequency range of 0.4 GHz, differences reaches 5 mm, 6 mm, and 14 mm for 0°, 35°, and 70°.

The obtained results indicate that even with the most intense impacts of solar hydrogen Lyα photons on the ionospheric D-region, changes in the propagation of the GNSS signal are significantly smaller than in periods of intense perturbations of this ionospheric layer caused by e.g. solar X-ray flares when P_D can exceed 1 m (Nina et al., 2020). However, for large values of θ parameter, the obtained P_D exceed 1 cm, which represents the minimum value that is included in the total signal delay in Wautelet (2013). For this reason, as well as the fact that the sunspot number can be higher than 120 (the maximum value of σ considered in this analysis), one can conclude that the positioning error that a quiet D-region at solar cycle maxima can cause is not negligible. In other words, variations in the hydrogen Lyα photons that arrive in this layer can provide enough large changes in propagation of a single GNSS signal that using of one GNSS signal and one receiver is not relevant for precise positioning, among others, due to the influence of the quiet D-region during intense radiation from the Sun.

Table 1. The signal delay P_D modelled for Waits parameters presented in Ferguson (1998) (Long Wavelength Propagation Capability (LWPC) numerical model), Bilitza (2018) (International Reference Ionosphere (IRI) model), Thomson et al. (2005), Han et al. (2011), McRae & Thomson (2000) and Thomson et al. (2017) for the signal zenith angle, θ, of 0°, 35°, and 70°, and GNSS signal frequencies, f, of 1.2 GHz and 1.6 GHz.

source of Wait's parameters	P_D ($\theta = 0°$)	P_D ($\theta = 35°$) (mm) $f = 1.2/1.6$ GHz	P_D ($\theta = 70°$)
Ferguson (1998)	0.44/0.25	0.54/0.30	1.29/0.72
Bilitza (2018)	1.59/0.89	1.94/1.09	4.65/2.61
Thomson et al. (2005)	3.77/2.12	4.61/2.59	11.04/6.21
Han et al. (2011)	8.98/5.05	10.97/6.17	26.27/14.78
McRae & Thomson (2000)	4.48/2.52	5.47/3.08	13.11/7.37
Thomson et al. (2017)	1.06/0.59	1.29/0.73	3.09/1.74

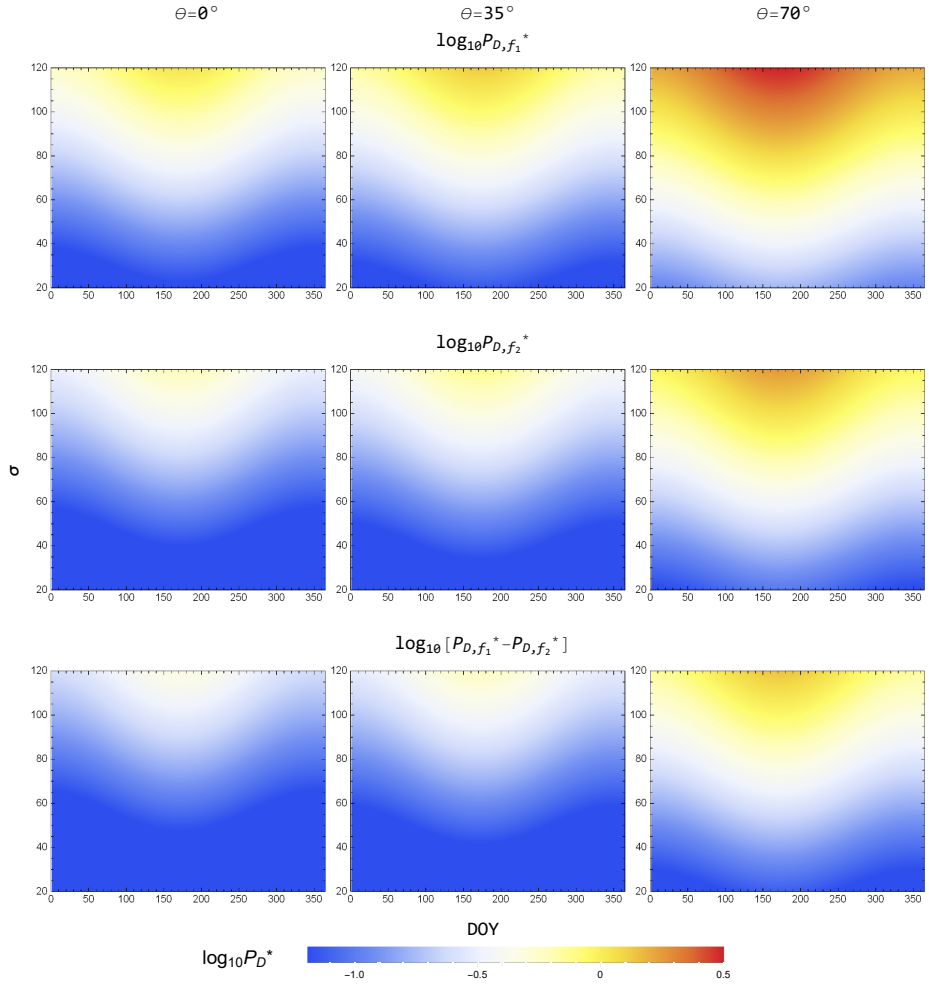

Figure 3. Dependencies of the GNSS signal delay logarithm ($\log_{10}(P_D^*)$ in the ionospheric D-region on the day of year, DOY, and the smoothed daily sunspot number σ. Here, $P_D^* = P_D/1\text{cm}$. The considered zenith angle of the signal are $\theta = 0°$ (first column), $\theta = 35°$ (second column), and $\theta = 70°$ (third column). First two rows represent the signal delay for the specific frequencies $f_1 = 1.2\,\text{GHz}$ and $f_2 = 1.6\,\text{GHz}$, and the third one represents the difference between those delays.

The obtained values of P_D are in good agreement with those modelled by the presented procedure for the values of Wait'a parameters given in Ferguson (1998) (Long Wavelength Propagation Capability (LWPC) numerical model), Bilitza (2018) (International Reference Ionosphere (IRI) model), Thomson et al.

(2005), Han et al. (2011), McRae & Thomson (2000) and Thomson et al. (2017). Namely, based on the data given in the Tab. 1, it can be seen that all the stated values are within the corresponding ranges obtained in this study.

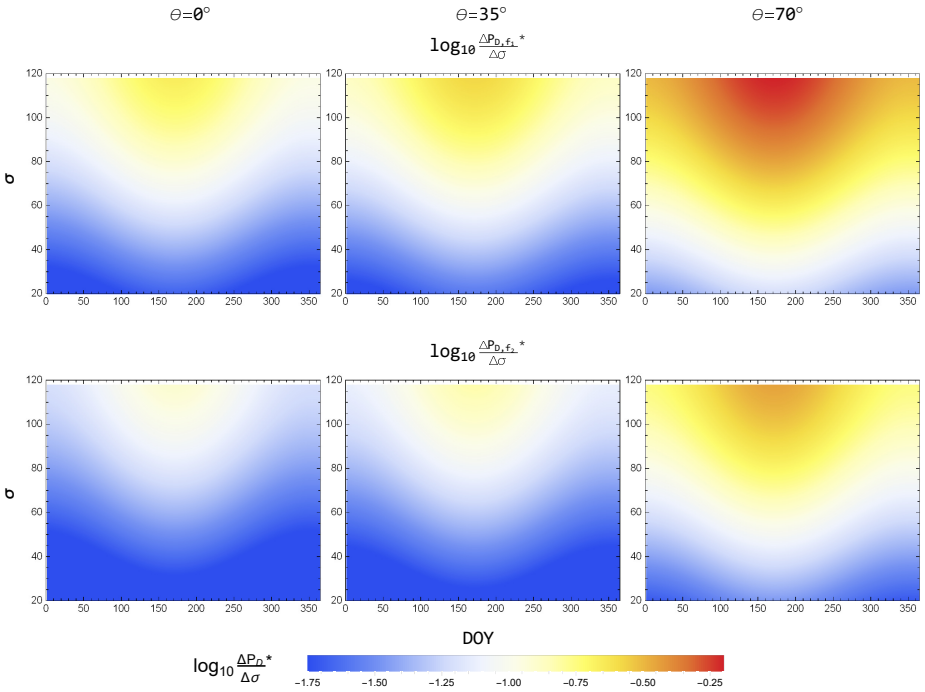

Figure 4. Dependencies of logarithm of the derivative of the GNSS signal delay in the ionospheric D-region with the smoothed daily sunspot number σ ($\log\frac{\Delta P_D^*}{\Delta\sigma}$) on the day of year, DOY, and σ. The considered zenith angle of the signal θ are $\theta = 0°$ (first column), $\theta = 35°$ (second column), and $\theta = 70°$ (third column). The rows represent the considered quantities for the specific frequencies $f_1 = 1.2\,\mathrm{GHz}$ and $f_2 = 1.6\,\mathrm{GHz}$.

In order to examine the influence of the changes in the solar hydrogen Lyα radiation intensity on changes in P_D, we present an analysis of the dependencies of $\frac{\Delta P_D}{\Delta\sigma}$ on DOY and σ. In Fig. 4, where this dependence is presented for the previously observed values of θ and f, it can be seen that the influence of changes in the sunspot number, i.e. the observed Lyα radiation, on the propagation of the GNSS signal is the greatest during the summer solstice and that it increases with θ. Also, it is important to emphasize that this influence is much more pronounced in the maximum than in the minimum of a solar cycle.

4. Conclusions

In this study, we present a study of the influence of a solar cycle (represented as the smoothed daily sunspot number) and season (represented as the day of year) period, on propagation of the GNSS signals, with the fixed frequency and incident zenith angle, in the ionospheric D-region. We perform the total electron content and signal delay in this ionospheric layer in order to investigate if influence of the quiet D-region can be ignored under all conditions.

The most important conclusion of this study is that variations in the hydrogen Lyα photons arriving in this layer can provide enough large changes in propagation of a single GNSS signal that using of one GNSS signal and one receiver is not relevant for precise positioning.

In addition, the obtained results show the following:

– The total electron content and signal delay increase with the zenith angle and the daily smoothed sunspot number. They are larger in the summer than in the winter months, and reached their maximum values during the summer solstice.

– The obtained signal delays are smaller than in periods of intense perturbations of this ionospheric layer caused by e.g. solar X-ray flares.

Furthermore, various initial conditions affect the ionospheric D-region differently, which consequently affects the propagation of the satellite signals. These influences will be the subject of future research.

Acknowledgements. The authors acknowledge funding provided by the Institute of Physics Belgrade and the Faculty of Civil Engineering, University of Belgrade, through the Ministry of Education, Science, and Technological Development of the Republic of Serbia grants.

References

Bilitza, D., IRI the International Standard for the Ionosphere. 2018, *Advances in Radio Science*, **16**, 1, DOI: 10.5194/ars-16-1-2018

Ferguson, J. A. 1998, *Computer Programs for Assessment of Long-Wavelength Radio Communications, Version 2.0*, ed. Space and Naval Warfare Systems Center, San Diego, CA

Han, F., Cummer, S. A., Li, J., & Lu, G., Daytime ionospheric D region sharpness derived from VLF radio atmospherics. 2011, *Journal of Geophysical Research (Space Physics)*, **116**, 5314, DOI: 10.1029/2010JA016299

Hofmann-Wellenhof, B., Lichtenegger, H., & Wasle, E. 2008, *GNSS Global Navigation Satellite Systems: GPS, GLONASS, Galileo, and more*, ed. Springer, Vienna, Austria

McRae, W. M. & Thomson, N. R., VLF phase and amplitude: daytime ionospheric parameters. 2000, *Journal of Atmospheric and Solar-Terrestrial Physics*, **62**, 609, DOI: 10.1016/S1364-6826(00)00027-4

Nina, A., Nico, G., Mitrović, S., et al., Quiet Ionospheric D-Region (QIonDR) Model Based on VLF/LF Observations. 2021, *Remote Sensing*, **13**, 483, DOI: 10.3390/rs13030483

Nina, A., Nico, G., Odalović, O., et al., GNSS and SAR Signal Delay in Perturbed Ionospheric D-Region During Solar X-Ray Flares. 2020, *IEEE Geoscience and Remote Sensing Letters*, **17**, 1198, DOI: 10.1109/LGRS.2019.2941643

Seeber, G. 2003, *Satellite Geodesy*, Walter de Gruyter, Berlin, Germany

Thomson, N. R., Experimental daytime VLF ionospheric parameters. 1993, *Journal of Atmospheric and Terrestrial Physics*, **55**, 173, DOI: 10.1016/0021-9169(93)90122-F

Thomson, N. R., Clilverd, M. A., & Rodger, C. J., Midlatitude ionospheric D region: Height, sharpness, and solar zenith angle. 2017, *Journal of Geophysical Research: Space Physics*, **122**, 8933, DOI: 10.1002/2017JA024455

Thomson, N. R., Rodger, C. J., & Clilverd, M. A., Large solar flares and their ionospheric D region enhancements. 2005, *Journal of Geophysical Research (Space Physics)*, **110**, A06306, DOI: 10.1029/2005JA011008

Todorović-Drakul, M., Čadež, V., Bajčetić, J., et al., Behaviour of electron content in the ionospheric D-region during solar X-ray flares. 2016, *Serbian Astronomical Journal*, **2016**, 11, DOI: 10.2298/SAJ160404006T

Wait, J. R. & Spies, K. P. 1964, *Characteristics of the Earth-ionosphere waveguide for VLF radio waves*, NBS Technical Note, CO

Wautelet, G. 2013, Characterization of Ionospheric Irregularities and Their Influence on High-Accuracy Positioning with GPS over Mid-Latitudes, Doctoral dissertation, University of Liège, Belgium